

Elsevier Editorial System(tm) for Journal of Photochemistry and Photobiology A:  
Chemistry  
Manuscript Draft

Manuscript Number: JPHOTOCHEM-D-14-00396R1

Title: Photoactive TiO<sub>2</sub>-montmorillonite composite for degradation of organic dyes in water

Article Type: Regular Article

Keywords: TiO<sub>2</sub>-montmorillonite; Composite; Photoactivity; Dye; Decolourization; Water

Corresponding Author: Dr. Claudia Letizia Bianchi,

Corresponding Author's Institution: Università degli Studi di Milano

First Author: R. Djellabi

Order of Authors: R. Djellabi; M.F. Ghorab; Giuseppina Cerrato; Sara Morandi; Sara Gatto; Valeria Oldani; Alessandro Di Michele; Claudia Letizia Bianchi

Abstract: TiO<sub>2</sub>-montmorillonite composite (TiO<sub>2</sub>-M) was prepared by impregnation with TiCl<sub>4</sub> followed by calcination at 350°C. The synthesized material was characterized by FTIR, TG-TDA, BET, XRD and SEM-EDX. The results show that TiO<sub>2</sub> was efficiently formed in Na- montmorillonite (Na-M) framework, and only a crystalline, pure anatase phase was produced. Photoactivity tests were carried out under UV-A irradiation using five selected organic dyes. The results indicate that the activity of TiO<sub>2</sub>-M is more important for cationic dyes, where the removal rates are in the order: Crystal violet (97.1%) > Methylene blue (93.20%) > Rhodamine B (79.8 %) > Methyl orange (36.1 %) > Congo red (22.6 %). The results of the TiO<sub>2</sub>-M activity were compared with that of the commercial P25. The comparison demonstrates that the synthesized TiO<sub>2</sub>-M exhibits a higher adsorptive behavior and can be used as low-cost alternative to the commercial TiO<sub>2</sub> for wastewater treatment, showing also an extreme easiness to completely recover the composite catalyst at the end of the test.



UNIVERSITÀ DEGLI STUDI DI MILANO  
DIPARTIMENTO DI CHIMICA

**Covering letter**

Manuscript title: **Photoactive TiO<sub>2</sub>-montmorillonite composite for degradation of organic dyes in water**

Corresponding author:

**Claudia Letizia Bianchi** (Department of Chemistry, University of Milan - Via Golgi 19, 20133 Milano, Italy - phone: +39 0250314253; e-mail: [Claudia.bianchi@unimi.it](mailto:Claudia.bianchi@unimi.it) ).

Type of manuscript: **Article**

Dear Mr. Editor,

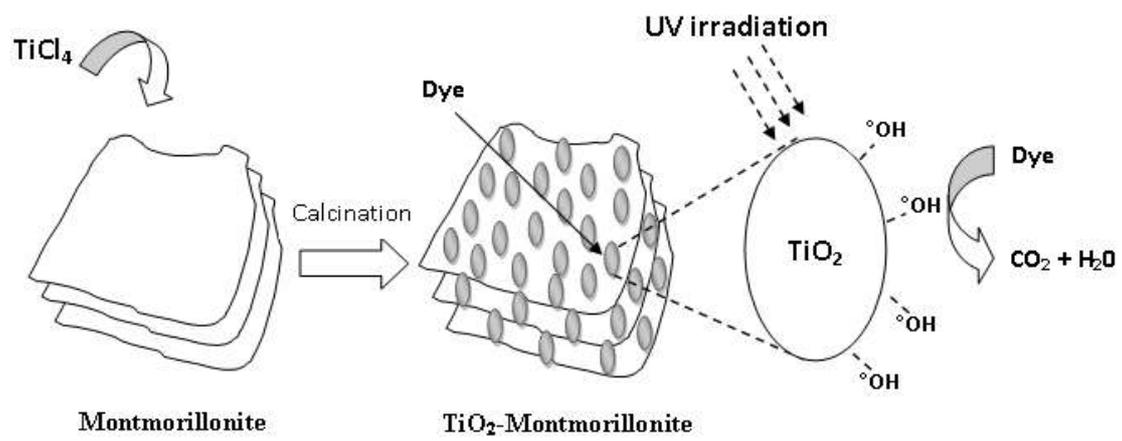
Please find enclosed the above mentioned manuscript, in which the preparation of a new composite TiO<sub>2</sub>-based material was reported. Sample features and photocatalytic results towards the photodegradation of organic dyes in water are also reported and commented. All results are compared to that of the reference commercial nano-sized P25 system. The paper is the first contribution of a recent collaboration between my group at the University of Milan and Prof.Ghorab's group in Algeria.

With my best regards,

Milano, June 24<sup>th</sup>, 2014

Prof. Claudia L. Bianchi

A handwritten signature in black ink, appearing to read 'Claudia L. Bianchi'.



## Highlights

- Preparation of TiO<sub>2</sub>-montmorillonite composite
- Photodecolourization of five dyes using TiO<sub>2</sub>-M and P25
- Comparison study between anionic and cationic dyes
- Full characterization of TiO<sub>2</sub>-montmorillonite

**Prof. Bernaurdshaw Neppolian<sup>a</sup>**

SRM Research Institute

SRM University, Kattankulathur

Chennai

India

Email: [b\\_neppolian@yahoo.com](mailto:b_neppolian@yahoo.com)

**Prof. Mathupandian Ashokkumar**

The School of Chemistry

University of Melbourne

Melbourne, Victoria 3010

Australia

email: [masho@unimelb.edu.au](mailto:masho@unimelb.edu.au)

**Prof. Vicente Cortes Corberan**

Institute of Catalysis and Petroleum chemistry (ICP), CSIC

Calle Marie Curie, 2, Cantoblanco, 28049 Madrid, Spain

email: [vcortes@icp.csic.es](mailto:vcortes@icp.csic.es)

Ms. Ref. No.: JPHOTOCHEM – D -14-00396

Dear Mr. Editor,

please find enclosed the revised version of our manuscript titled: “Photoactive TiO<sub>2</sub>-montmorillonite composite for degradation of organic dyes in water” by R. Djellabi, M. F. Ghorab, G.Cerrato, S. Morandi, S. Gatto, V. Oldani, A. Di Michele, C.L. Bianchi.

All suggestions and comments by the Reviewers have been fully considered and modifications have been introduced in the manuscript, accordingly.

A detailed point by point list of our replies was prepared.

Best Regards

Prof. Claudia Bianchi

## Reviewer 1

The authors are grateful to the Referee for the pertinent and helpful comments. All the recommendations have been seriously considered and revisions have been introduced in the manuscript, accordingly.

1) Without any specific example, a thorough revision on the use of English as well as grammar and spell check is recommended.  
English was completely revised by a mother-tongue colleague.

2) BET surface area TiO<sub>2</sub> P25 Evonik as 49 m<sup>2</sup>/g should be supported by a reference. A new ref (n. 28) was added into the text.

3) pH dependent evaluation of the substrate properties should be presented.  
pH is around 6.5 for started solutions. This datum was added into the text in the Experimental section.  
No other evaluations on the pH during the degradation steps were made at present.

4) Photocatalytic tests: Fig.2. should be revised.  
Fig.2 was redrawn in order to clarify the photoreactor.

5) Methodology for the determination of the residual concentration of the dyes should be explained.  
The details of the determination of the residual concentration were added to the text:  
The removal rate of the dyes was calculated using the following equation:

$$R(\%) = \frac{(C_0 - C_t)}{C_0} \times 100 \quad (1)$$

Where  $C_0$  and  $C_t$  represent the dye concentration (mol/L) before and after reaction.

6) Fig.4. should be revised, not clearly presented.  
Figure 4 was redrawn to be clearer.

7) Table 2. should also cover TiO<sub>2</sub> properties.  
We cannot satisfy this request because we did not prepare bare TiO<sub>2</sub>, but TiO<sub>2</sub> was only embedded into the montmorillonite framework. The pure TiO<sub>2</sub> used to compare our results was the well-known P25 by Evonik, commonly used as reference material for photocatalyst both in liquid and gas phase tests.

8) Figure captions should be revised.  
Figure captions were revised.

9) Table 3. should be revised and explained in detail.  
Table 3 summarizes the same results of figures from 7 to 11 in order to facilitate the comparison. A new sentence was added into the text to clarify this point.

## Reviewer 2

The authors are grateful to the Referee for the pertinent and helpful comments. All the recommendations have been seriously considered and revisions have been introduced in the manuscript, accordingly.

1. Equations 1 and 2 are well known and not necessary. The authors should remove the equations in the revised manuscript.

Eqs 1 and 2 have been removed from the text.

2. Typographical errors are present in many places

All typographical errors have been corrected in the text.

3. Fig. 6 EDX spectrum is also not necessary as Table 2 is enough for the manuscript  
EDX spectrum has been removed from Fig. 6.

4. It is very important to know whether the % degraded values are excluded or included the % adsorption values or not? It should be explained clearly to know the total degradation of the dyes.

These details have been added into the text.

5. The dissimilarity observed between P25 and TiO<sub>2</sub>-M on the adsorption rate of dyes can be explained by the different properties and morphologies of these materials. The surface of TiO<sub>2</sub>-M, both internal and external, is porous and spongy, on the contrary TiO<sub>2</sub> P25 particles exhibit a smooth surface. Furthermore, the high cation exchange capacity of TiO<sub>2</sub>-M due to negative charge in its interlayer increases the attraction and the adsorption of cationic dyes [39]. In addition, the point of zero charge (PZC) of TiO<sub>2</sub> P25 is reported to be in the pH range of 6-7.5 [40] which is near to our pH range working. At this point, the surface charge is null thus resulting to be less attractive to the dye molecules.

Two references were also added.

6. The authors should describe that why there are dissimilarities between P-25 and TiO<sub>2</sub>-M on the % adsorption of the dyes

It is important to note that the adsorption behavior of this material contributes simultaneously to accelerate the photocatalytic action and to participate for the total removal of dyes. Hence, the total degradation rate of dyes should include an adsorption part of dye especially when dye molecules are accumulated inside the pores of TiO<sub>2</sub>-M. In this case, UV irradiation and produced radicals cannot reach them. Furthermore, it is difficult to evaluate the adsorption contribution in the degradation rate, but we can ensure that this material combines the adsorption and the photocatalytic reaction to remove dyes from water.

# Photoactive TiO<sub>2</sub>-montmorillonite composite for degradation of organic dyes in water

R. Djellabi<sup>a</sup>, M. F. Ghorab<sup>a</sup>, G. Cerrato<sup>c</sup>, S. Morandi<sup>c</sup>, S. Gatto<sup>b</sup>, V. Oldani<sup>b</sup>, A. Di Michele<sup>d</sup>, C.L. Bianchi<sup>b\*</sup>

<sup>a</sup>Laboratory of Water Treatment and Valorization of Industrial Wastes, Chemistry Department, Faculty of Sciences, Badji-Mokhtar University, BP12 2300, Annaba, Algeria

<sup>b</sup>Università degli Studi di Milano & Consorzio INSTM-UdR Milano, Dip.Chimica, Via Golgi, 19 – 20133 Milano, Italy

<sup>c</sup>Università degli Studi di Torino, Dipartimento di Chimica & NIS Interdept. Centre & Consorzio INSTM-UdR Torino, Via Giuria, 7 – 10125 Torino, Italy

<sup>d</sup>Università degli Studi di Perugia, Dipartimento di Fisica e Geologia, Via Pascoli – 06123 Perugia, Italy

Corresponding author: [claudia.bianchi@unimi.it](mailto:claudia.bianchi@unimi.it)

## Abstract

TiO<sub>2</sub>-montmorillonite composite (TiO<sub>2</sub>-M) was prepared by impregnation with TiCl<sub>4</sub> followed by calcination at 350°C. The synthesized material was characterized by FTIR, TG-TDA, BET, XRD and SEM-EDX. The results show that TiO<sub>2</sub> was efficiently formed in Na-montmorillonite (Na-M) framework, and only a crystalline, pure anatase phase was produced. Photoactivity tests were carried out under UV-A irradiation using five selected organic dyes. The results indicate that the activity of TiO<sub>2</sub>-M is more important for cationic dyes, where the removal rates are in the order: Crystal violet (97.1%) > Methylene blue (93.20%) > Rhodamine B (79.8 %) > Methyl orange (36.1 %) > Congo red (22.6 %). The results of the TiO<sub>2</sub>-M activity were compared with that of the commercial P25. The comparison demonstrates that the synthesized TiO<sub>2</sub>-M exhibits a higher adsorptive behavior and can be used as low-cost alternative to the commercial TiO<sub>2</sub> for wastewater treatment, showing also an extreme easiness to completely recover the composite catalyst at the end of the test.

**Keywords:** TiO<sub>2</sub>-montmorillonite; Composite; Photoactivity; Dye; Decolourization; Water.

## 1. Introduction

Heterogeneous photocatalysis is becoming more interesting in recent years for several research areas, especially, for environmental applications [1, 2]. Among these applications, water remediation and in particular the decolourization of wastewaters is one of the most important area where scientific research has been focused [3, 4]. Among different kinds of photocatalysts, TiO<sub>2</sub> has been the most widely used for wastewater treatment because of its strong oxidizing properties for the removal of organic pollutants, super-hydrophilicity and chemical stability [1, 5]. It is known that the optical properties of TiO<sub>2</sub> and, as a consequence, its photoactivity, are strongly influenced by its characteristics like structure, morphology, particles size. For this purpose, many researchers have developed several methods for the preparation of new TiO<sub>2</sub> photocatalysts, with tailored features aimed at improving the final photoactivity towards the degradation of pollutants both in gas and water phase: TiO<sub>2</sub> nanopowders [6-8], N-doped carbon-TiO<sub>2</sub> [9, 10], doping of TiO<sub>2</sub> by transition metals [11] or noble metals [12] and TiO<sub>2</sub> in conjunction with other semiconductors [13-15].

Moreover, the photoactivity performances are strongly depended on the adsorption capacity of the photocatalyst, as it is known that the photocatalytic reaction occurs on the photocatalyst surface [16]. In order to improve the adsorption process, the immobilization of TiO<sub>2</sub> on porous materials like natural clays is a successful method. Furthermore, Ooka *et al.* reported that TiO<sub>2</sub>/clay composites exhibit the advantage to photodecompose organic pollutants in water due to their hydrophobic interlayers [17]. TiO<sub>2</sub>/clay composites have been synthesized by deposition (or pillaring) TiO<sub>2</sub> particles either on the surface of the clays or into their interlayers, thus obtaining dispersed TiO<sub>2</sub> nanoparticles with a high photoactivity. Different kinds of clays have been used. These included sepiolite [18], bentonite [19], kaolinite [20], zeolite [21] and montmorillonite [22]. Moreover, several methods have been used for the synthesis of TiO<sub>2</sub>/clay composites. Such methods include the TiCl<sub>4</sub> adsorption followed by

calcination [23], sol-gel synthesis [24],  $\text{TiCl}_4$  hydrolysis [25] and by wet grinding in an agate mill [26].

In the present work, a  $\text{TiO}_2$ -montmorillonite composite ( $\text{TiO}_2$ -M) was synthesized using a natural Na-montmorillonite impregnated with  $\text{TiCl}_4$  and followed by calcination. Physico-chemical properties of the photocatalyst were determined by FTIR spectroscopy, TG-TDA, BET, XRD and SEM-EDX, whereas photoactivity was evaluated using five selected organic dyes in aqueous solution under UV-A irradiation. Photoactivity results were compared with those obtained employing the P25 by Evonik, a commercial sample often used as reference material in photocatalysis.

## **2. Materials and methods**

### **2.1. Materials**

The montmorillonite used in this study was a natural sodium-exchanged bentonite (Na-M) from the Roussel deposit in Maghnia (Algeria) and was used without any further treatment or purification. The cationic exchange capacity of Na-M, determined by methylene blue method [27], is 89.30 mmol/100 g.

$\text{TiO}_2$  P25 (Evonik) was used in the present study as a reference material. It is composed of approximately 80% anatase and 20% rutile, a BET surface area of 49  $\text{m}^2/\text{g}$  and with crystallites size of about 25 nm [28].

Dyes used in this work were Cristal violet (Fluka), Rhodamine B (SIGMA-ALDRICH), Congo red (Fluka), Methylene blue (Fluka) and Methyl orange (SIGMA-ALDRICH). The structure of each dye is presented in Figure 1.

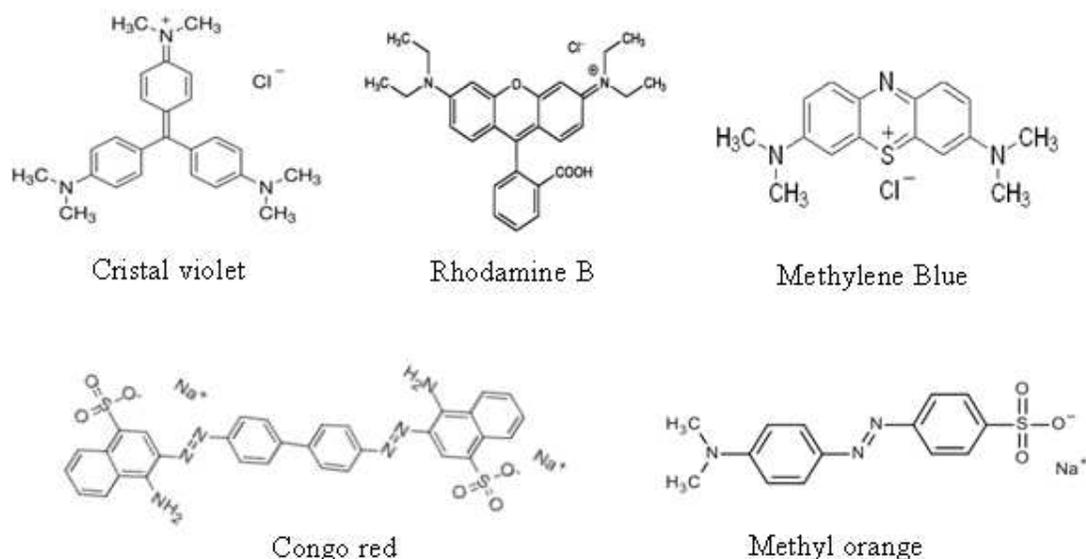


**Figure 1.** Chemical structure of different dyes used in this study

## 2.2. Synthesis of titania-montmorillonite

The photocatalyst synthesis method was similar to that reported by Rossetto *et al.*[29]. Titania-montmorillonite ( $\text{TiO}_2\text{-M}$ ) was prepared by impregnation with  $\text{TiCl}_4$  (Aldrich, 99.99%). Firstly,  $\text{TiCl}_4$  was diluted with  $\text{CH}_2\text{Cl}_2$  to obtain a clear solution. Then, the mixture was slowly added to Na-M suspension under vigorous stirring at  $65^\circ\text{C}$  for 4 hours under reflux system. The weight ratio of Ti/montmorillonite was 10% (g/g). The wet solid obtained was washed by double-distilled water, filtered and then dried at  $110^\circ\text{C}$  for 24 h: finally, it was calcined in air at  $350^\circ\text{C}$  for 4 h. The final sample, immersed in water, shows a pH of 6.5.

## 2.3. Characterization

Fourier Transform InfraRed (FT-IR) spectra of Na-M and  $\text{TiO}_2\text{-M}$  (as self-supporting pellets,  $\sim 20 \text{ mg cm}^{-2}$ ) were recorded at room temperature at a  $2 \text{ cm}^{-1}$  resolution in the  $4000\text{-}400 \text{ cm}^{-1}$  spectral range using a Perkin–Elmer FT-IR System 2000 spectrophotometer, equipped with a

Hg–Cd–Te cryo-detector. The self-supporting pellets were posed in a quartz cell equipped with KBr windows: before recording the FTIR spectra, all samples have been activated in vacuo connecting the cell to a vacuum line (residual pressure  $< 10^{-4}$  mbar). Thermogravimetry-Differential Thermal Analysis (TG-DTA) was performed using a thermogravimetric analyzer (NETZSCH STA 409 PC/PG) at a heat rate of  $10^{\circ}\text{C}/\text{min}$  from 25 to  $500^{\circ}\text{C}$  under air atmosphere.

The BET specific surface areas were determined using a Thermo Quest Sorptomatic 1990 Technical Specification instrument.

The morphology of Na-M and  $\text{TiO}_2$ -M particles was determined by Field Emission Scanning Electron Microscopy (FEG LEO 1525, ZEISS Company, Germany). The Energy Dispersion X-ray Spectroscopy (EDS) analysis (Quantax 200 with Xflash 400 detector, Bruker Company, Germany), coupled with the Scanning Electron Microscopy, was used to analyze the elements content of the samples.

The XRD patterns were recorded on a diffractometer instrument (Philips PW3830/3020 X'Pert diffractometer, PANalytical) using monochromatized  $\text{CuK}\alpha$  radiation at  $\lambda = 1.54 \text{ \AA}$ . The interlayer d-spacing reflection was calculated using the Bragg equation [30]. The crystallite size of anatase  $\text{TiO}_2$  was calculated using Scherrer's formula.

### **3.4. Photocatalytic tests**

The photocatalytic experiments were carried out in a static quartz reactor (500 mL), equipped with a cold finger to avoid thermal reactions (Figure 2). A UV-A lamp ( $\lambda_{\text{max}} = 365\text{nm}$ ,  $100\text{W}/\text{m}^2$ ) was placed next to the reactor at 10 cm. In a typical experiment, 0.08 g of the photocatalyst and 500 mL of dye solution at  $10^{-4}$  mol/L were stirred under irradiation for 6 h. During the reaction, samples were collected at selected time intervals. The adsorption experiments were performed under the same conditions without irradiation. The powdered

photocatalysts were removed by filtration (0.45  $\mu\text{m}$ , Whatman) and the residual concentration of dyes was determined using a UV–visible spectrophotometer (T60 PG Instruments).

The removal rate of the dyes was calculated using the following equation:

$$R(\%) = \frac{(C_0 - C_t)}{C_0} \times 100 \quad (1)$$

Where  $C_0$  and  $C_t$  represent the dye concentration (mol/L) before and after reaction.

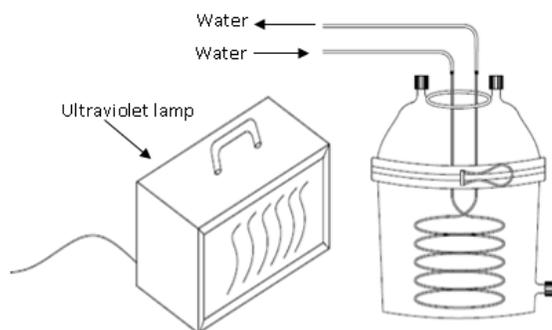


**Figure 2.** Scheme of the photoreactor

### 3. Results and discussion

#### 3.1. Physico-chemical characterization

##### 3.1.1. FTIR

Figure 3 shows the FTIR spectra (in the 4000-1200  $\text{cm}^{-1}$  range) of Na-M and  $\text{TiO}_2$ -M obtained after activation *in vacuo* at room temperature (RT).

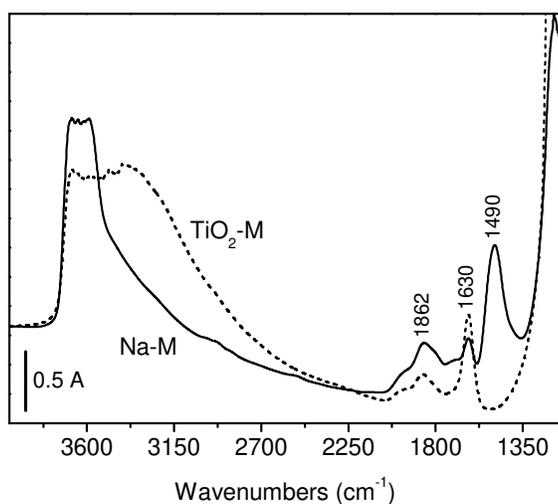


**Figure 3.** FTIR spectra of Na-M and TiO<sub>2</sub>-M after activation in vacuo at RT.

For both samples, there are present bands in the 3700-3000 cm<sup>-1</sup> range: on the basis of their spectral behavior and of literature data [31-33], they can be assigned to the stretching vibration modes of all (either structural and/or surface) OH groups mutually interacting by H-bonding. The spectroscopic counter part of these modes can be observed at ~1630 cm<sup>-1</sup>: it corresponds to the bending mode of all undissociated H<sub>2</sub>O molecules present in/on the materials. Moreover, in the 2000-1700 cm<sup>-1</sup> range a complex envelope of bands is present for both materials: it can be assigned to the typical overtones of the SiO<sub>2</sub>-like matrix [34]. On the other hand, it is worth noting that Na-M exhibits a sharp and complex spectral component at ~1490 cm<sup>-1</sup>: this component, totally absent in the case of TiO<sub>2</sub>-M, is ascribable to some modes typical of carbonate anions [35]. The absence of this component in the TiO<sub>2</sub>-containing material can be related to the addition of TiO<sub>2</sub>, as reasonably in the synthetic step the anions present in the interlayers of the montmorillonite material are totally substituted by the anions formed by titanium-containing species. In the calcination step, the presence of the latter

species brings about the formation of  $\text{TiO}_2$  and leads to the retaining of a higher amount of water, as evidenced in  $\text{TiO}_2$ -M spectrum reported in Figure 3: the envelope assigned to the OH stretching mode and the component located at  $1630\text{ cm}^{-1}$  (bending mode of undissociated molecular water) are much larger/more intense in the case of  $\text{TiO}_2$ -M.

### 3.1.2. TG/DTA

The TG/DTA curves of Na-M and  $\text{TiO}_2$ -M samples in the temperature range from 25 to 500 °C are reported in Figure 4. The TG curve shows weight loss in two stages of 25-200 and 200-500°C for both samples. The first stage corresponds to a weight loss of 11.18 and 5.66 % for Na-M and  $\text{TiO}_2$ -M, respectively. This mass change is due to the evaporation of physisorbed water [24, 36]. The DTA curve exhibits endothermic peaks at 99.5 °C (Na-M) and 105.4 °C ( $\text{TiO}_2$ -M) which confirms the loss of adsorbed water. The lower mass change in the case of  $\text{TiO}_2$ -M, if compared to Na-M, can be related to the presence of  $\text{TiO}_2$  itself, and also confirmed by the major amount of OH groups observed in the FTIR spectra after activation *in vacuo* (see Figure 3). The second stage shows a lower weight loss of 0.50% and 1.03% for Na-M and  $\text{TiO}_2$ -M, respectively. This is due to desorption of more strongly adsorbed water [37].

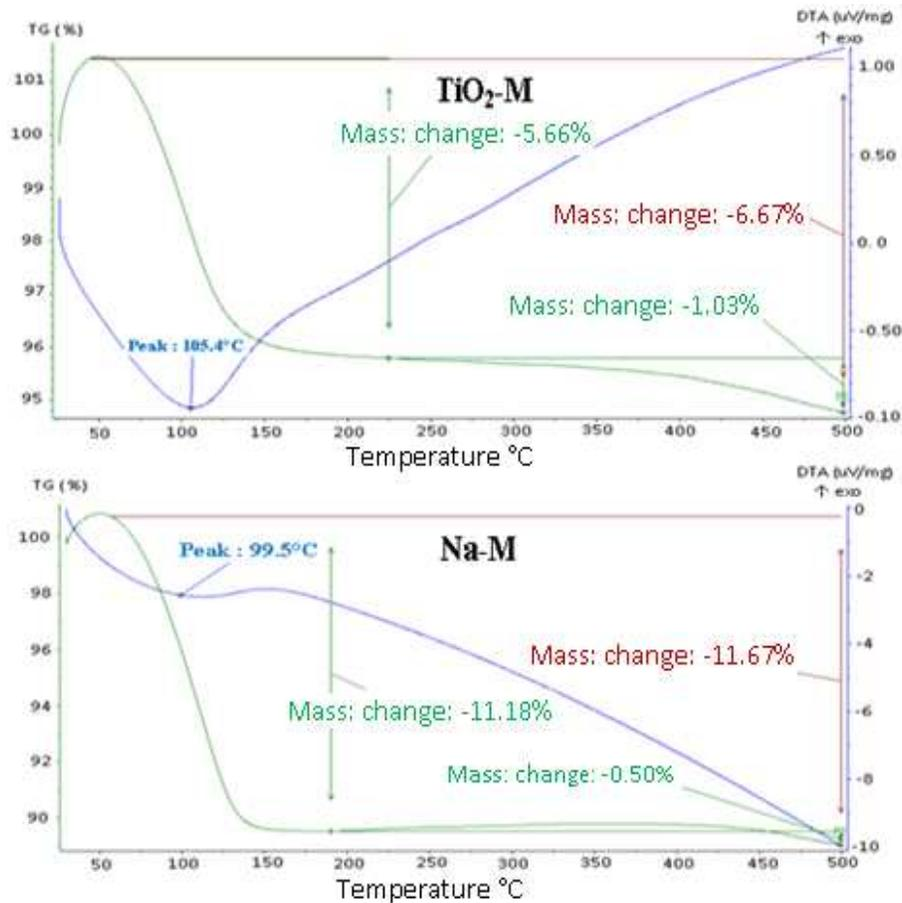


**Figure 4.** TG/DTA of Na-M and TiO<sub>2</sub>-M samples

### 3.1.3. Specific surface area and porosity measurements

The BET specific surface area of the Na-M and TiO<sub>2</sub>-M samples is shown in Table 1. It can be seen that the introduction of TiO<sub>2</sub> changes to a very limited extent the value of surface area of the starting material (49.4 to 51.5 m<sup>2</sup>/g). The change of the pore volume is more evident (from 0.107 to 0.144 cm<sup>3</sup>/g): it might be related to the addition of TiO<sub>2</sub>. As a matter of fact, for both samples the isotherms related to adsorption/desorption branch of N<sub>2</sub> at 77K exhibit the shape typical of mesoporous materials and belong to type 2, with an evident hysteresis loop of type H<sub>3</sub> [38]. Moreover, if we analyse these data applying the BJH method, we can

preliminary conclude that both materials exhibit a net mesoporosity with a medium pore width of  $\sim 40$  Å.

**Table 1** Result of adsorption–desorption measurements

Samples	Specific surface area ( $\text{m}^2/\text{g}$ )	Pore volume ( $\text{cm}^3/\text{g}$ )
Na-M	49.4	0.107
TiO <sub>2</sub> -M	51.5	0.144

#### 3.1.4. XRD

The XRD patterns of Na-M and TiO<sub>2</sub>-M samples are reported in Figure 5. The small angle XRD pattern of Na-M shows a strong peak at  $2\theta=5.87^\circ$  due to the d(100) basal spacing reflection of the montmorillonite [39]. In the case of the TiO<sub>2</sub>-M sample, this peak is split into two components located at  $2\theta = 5.68^\circ$  and  $7.47^\circ$ : this splitting is a clear indication that the introduction of TiO<sub>2</sub> brings about a decreasing of the basal spacing of a part of the montmorillonitic material. The latter result demonstrates that the titanium species are really inserted in the montmorillonite interlayers. On the wide-angle diffraction, in the TiO<sub>2</sub>-M diffractogram we observe the typical peaks ascribable to a montmorillonite material; moreover, titanium crystallization reflections are also observed, in which only the anatase polymorph is evidenced. The average crystallite size of anatase was estimated of  $\sim 15$ -20 nm employing the (101) reflex for the calculation.

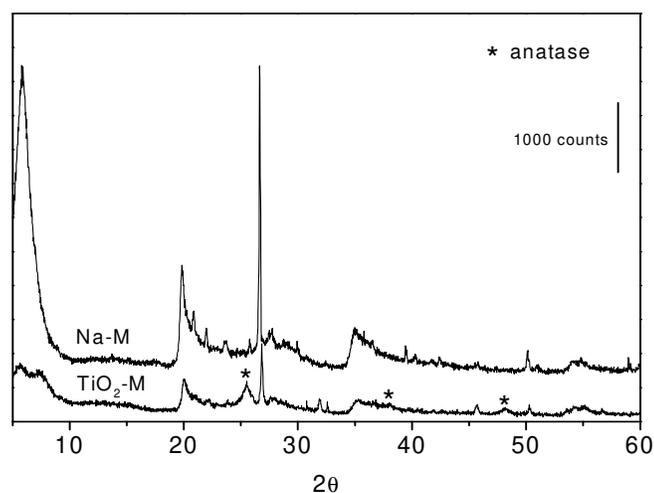


**Figure 5.** XRD patterns of Na-M and TiO<sub>2</sub>-M samples.

### 3.1.5. SEM-EDX

Figure 6 reports the SEM images of Na-M and TiO<sub>2</sub>-M. The Na-M sample has a spongy integrated flakes-like structure; furthermore, it exhibits some smooth regions in its structure. The TiO<sub>2</sub>-M image shows a clear change of the montmorillonite morphology: this feature can be ascribed to the decreasing of the interlayer spacing brought about by the addition of TiO<sub>2</sub>, as also indicated by the XRD characterization.

The results of the EDS analysis of Na-M and TiO<sub>2</sub>-M are reported as numerical values in Table 2. The results of the elemental analysis of Na-M indicate that Si and Al are the main constituents of the material, which are estimated to be 60.06 and 20.81 wt%, respectively. Furthermore, Na content in Na-M is larger than that of Ca. The content of Ti element in TiO<sub>2</sub>-M is 48.6 wt%. The high Ti content observed is much more than that added from TiCl<sub>4</sub> during the preparation (which was only 10 wt %). This is related to the calcination step operated at 350°C: as revealed by TG/DTA measurements, the loss of both adsorbed and structural water justifies the observed increasing of the Ti content [22].

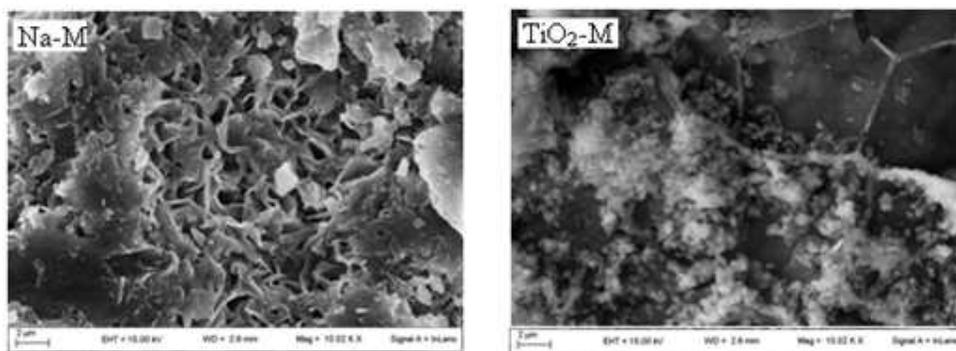


**Figure 6.** SEM images of Na-M (left-hand section) and TiO<sub>2</sub>-M (right-hand section) samples.

**Table 2** Elemental analysis of Na-M and TiO<sub>2</sub>-M

Element [w%]	Si	K	Al	Mg	Fe	Na	Ca	Cl	Ti
Na-M	60.06	1.03	20.81	5.37	6.07	4.84	1.25	0.57	-
TiO <sub>2</sub> -M	25.26	1.27	8.58	1.64	2.24	3.25	1.48	7.72	48.56

### 3.2. Photocatalytic activity

The results of the decolourization of different dyes using both P25 and TiO<sub>2</sub>-M under UV-A irradiation compared with direct photolysis and dark adsorption are reported in Figures 7-11 and also summarized in Table 3. Furthermore, the removal rates of different dyes are summarized in Table 3. From these results it can be observed that, after 6 h, the direct photolysis was different for each dye and was in the order: Methylene blue (20.6 %) > Rhodamine B (10.3 %) > Congo red (6.2 %) > Crystal violet (5.7 %) > Methyl orange (4.4 %).

The results of the dark adsorption on the P25 were in the range of 6.0 % to 18.6 %, where the Congo red and the Crystal violet possess the highest values. The photodegradation rates of

dyes by P25 were higher than 80% except for the Methyl orange (59.6 %). In the case of TiO<sub>2</sub>-M, the dark adsorption effectiveness of the same dyes follows the order: Methylene blue (67.6 %) > Crystal violet (58.8 %) > Rhodamine B (45.0 %) > Methyl orange (14.9 %) > Congo red (6.2 %), reflecting the higher adsorptive capacity of the cationic dyes (Methylene blue, Crystal violet and Rhodamine B). On the other hand, the anionic dyes show a smaller adsorption. This is due to less attraction charges of TiO<sub>2</sub>-M for the anionic dyes. The dissimilarity observed between P25 and TiO<sub>2</sub>-M on the adsorption rate of dyes can be explained by the different properties and morphologies of these materials. The surface of TiO<sub>2</sub>-M is porous and spongy, on the contrary TiO<sub>2</sub> P25 particles exhibit a smooth surface. Furthermore, the high cation exchange capacity of TiO<sub>2</sub>-M due to negative charge in its interlayer increases the attraction and the adsorption of cationic dyes [40]. In addition, the point of zero charge (PZC) of TiO<sub>2</sub> P25 is reported to be in the pH range of 6-7.5 [41], which is near to our pH range working. At this point, the surface charge is null thus resulting to be less attractive to the dye molecules.

The photodegradation of dyes by TiO<sub>2</sub>-M is in the order: Crystal violet (97.1 %) > Methylene blue (93.2 %)>Rhodamine B (79.8 %) > Methyl orange (36.1 %) > Congo red (22.6 %). It is worth mentioning the similarity in the orders obtained in the adsorption and photodegradation of the dyes under investigation. These results confirm the relationship between the adsorption and the photocatalytic activity, as the photodegradation reaction of organic pollutants occurs after their adsorption on the surface [40]. It is important to note that the adsorption behavior of this material contributes simultaneously to accelerate the photocatalytic action and to participate for the total removal of dyes. Hence, the total degradation rate of dyes should include an adsorption part of dye especially when dye molecules are accumulated inside the pores of TiO<sub>2</sub>-M: in this case, UV irradiation and produced radicals cannot reach them. Furthermore, it is difficult to evaluate the adsorption contribution in the degradation rate, but

we can ensure that this material combines the adsorption and the photocatalytic reaction to remove dyes from water.

The comparison between P25 and the synthesized TiO<sub>2</sub>-M composite demonstrates the advantages of this latter with a high adsorptive behavior and a cation exchange capacity of 96.5 mmol/100g, which favours the adsorption of a larger number of dye molecules. Consequently, it facilitates their degradation by the photoactive deposited TiO<sub>2</sub> particles, leading to a higher concentration of dye molecules around the TiO<sub>2</sub> particles as compared to that in the bulk solution, resulting in an increase in the degradation rate [42-43]. In addition, the adsorptive behavior of TiO<sub>2</sub>-M may contribute to the fixation of the intermediates produced during the degradation in order to be further oxidized.

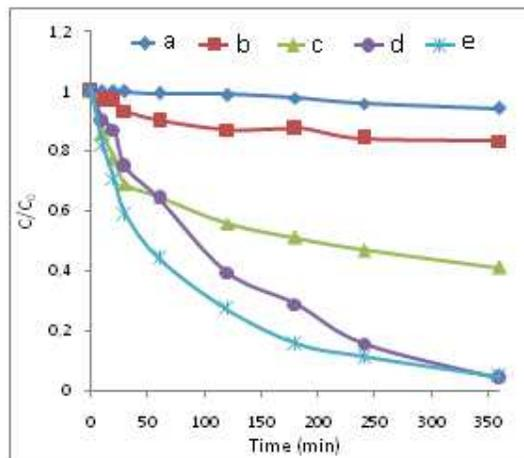


**Figure 7.** Photocatalytic decolorization of Crystal violet. (a):photolysis, (b):P25 (dark), (c): TiO<sub>2</sub>-M (dark), (d): P25 (UV), (e): TiO<sub>2</sub>-M (UV).

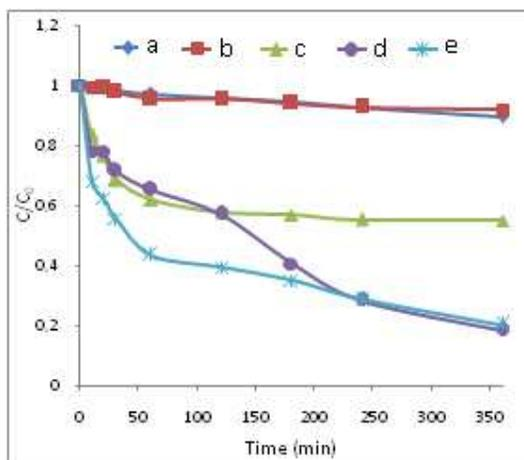


**Figure 8.** Photocatalytic decolorization of Rhodamine B. (a): photolysis, (b):P25 (dark), (c): TiO<sub>2</sub>-M (dark), (d): P25 (UV), (e): TiO<sub>2</sub>-M (UV).

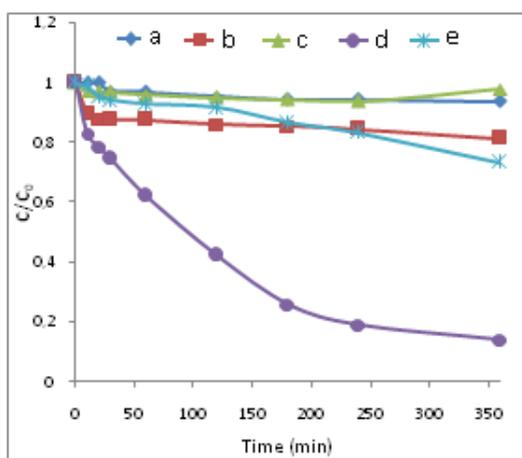


**Figure 9.** Photocatalytic decolorization of Congo red. (a): photolysis, (b):P25 (dark), (c): TiO<sub>2</sub>-M (dark), (d): P25 (UV), (e): TiO<sub>2</sub>-M (UV).

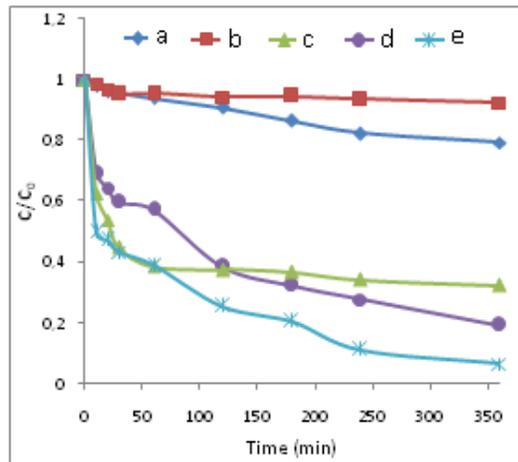


**Figure 10.** Photocatalytic decolorization of Methylene blue. (a):photolysis, (b): P25 (dark), (c): TiO<sub>2</sub>-M (dark), (d): P25 (UV), (e): TiO<sub>2</sub>-M (UV).

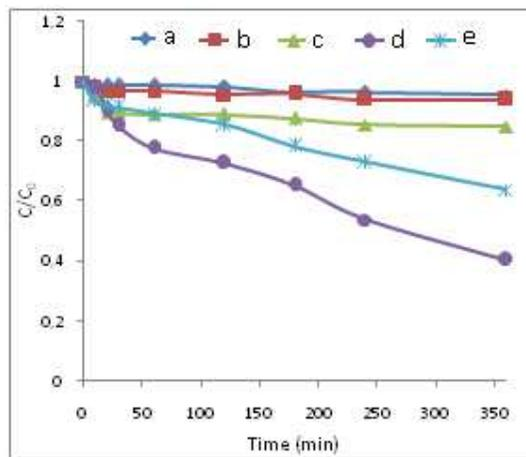


**Figure 11.** Photocatalytic decolorization of Methyl Orange. (a):photolysis, (b):P25 (dark), (c): TiO<sub>2</sub>-M (dark), (d): P25 (UV), (e): TiO<sub>2</sub>-M (UV).

**Table 3.** Comparison of the removal rates of different dyes using P25 and TiO<sub>2</sub>-M

		<b>Removal rate (%)</b>				
		Crystal violet	Congo red	Methylene blue	Methyl orange	Rhodamine B
	Photolysis	5.7	6.2	20.6	4.4	10.3
P25	In dark	16.5	18.6	7.6	6.0	8.1
	Under UV	95.8	85.9	80.7	59.6	81.2
TiO <sub>2</sub> -M	In dark	58.8	6.2	67.6	14.9	45.0
	Under UV	97.1	22.6	93.2	36.1	79.8

#### 4. Conclusions

TiO<sub>2</sub>-montmorillonite was synthesized using a simple method that consists in the impregnation of the clay with TiCl<sub>4</sub> followed by calcination.

The characterization results show that TiO<sub>2</sub> particles were, at least in part, introduced in the interlayer spaces of the montmorillonite. The Ti content in TiO<sub>2</sub>-M was 48.6 wt% with an anatase crystallite size of about 15-20 nm. The adsorption effectiveness and the photocatalytic degradation reactions of TiO<sub>2</sub>-M were more pronounced for the cationic dyes. Additionally, the photoactivity of TiO<sub>2</sub>-M increases when the dye molecules are more adsorbed: this is due to the increase of the contact between the TiO<sub>2</sub> particles deposited on the TiO<sub>2</sub>-M surface and the dye molecules.

The use of TiO<sub>2</sub>-M composite for water treatment is an attractive alternative to the commercial TiO<sub>2</sub> taking into account the higher adsorptive behavior, its low-cost and its rapid recovery at the end of the test by simple filtration as well.

## References

- [1] K.Nakata, A. Fujishima, TiO<sub>2</sub> photocatalysis: Design and applications, *J.Photochem.Photobiol. C*. 13 (2012) 169–189.
- [2] M.R., Hoffmann, S.T. Martin, W.Choi, D.W.Bahnmann, Environmental applications of semiconductor photocatalysis, *Chem. Rev.* 95(1) (1995) 69-96.
- [3] J-M.Herrmann, Heterogeneous photocatalysis: fundamentals and applications to the removal of various types of aqueous pollutants, *Catal. Today* 53 (1999) 115–129.
- [4] K. Kavita, C.Rubina, L.S. Rameshwar, Treatment of hazardous organic and inorganic compounds through aqueous-phase photocatalysis: a review, *Industrial Eng in. Chem. Res.* 43(2004) 7383–7696.
- [5] V.A. Sakkas, I.M. Arabatzis, I.K. Konstantinou, A.D. Dimou Albanis, P. Falaras, Metolachlor photocatalytic degradation using TiO<sub>2</sub> photocatalysts, *App.Catal. B: Environ.* 49 (2004) 195–20.
- [6] A.Hosseinnia, M.Keyanpour-Rad, M.Kazemzad, M.Pazouki, A novel approach for preparation of highly crystalline anatase TiO<sub>2</sub> nanopowders from the agglomerates, *Powder Technol.* 190 (2009) 390–392.
- [7] M. Caplovicová, P. Billik, L. ĀCaplovic, V. Brezová, T. Turáni, G. Plesch, P. Fejdi, On the true morphology of highly photoactive anatase TiO<sub>2</sub> nanocrystals. *App. Catal.B: Environ.* 117-118(2012) 224–235.
- [8] S.Ardizzone, C.L. Bianchi, G.Cappelletti, S. Gialanella, C. Pirola, V. Ragaini, Tailored anatase/brookitenanocrystalline TiO<sub>2</sub>. The optimal particle features for liquid- and gas-phase photocatalytic reactions, *J. Phys.Chem.C* 111 (2007) 13222-13231.

- [9] H. Ming, H. Huang, K. Pan, H. Li, Y. Liu, Z. Kang, C/TiO<sub>2</sub> nanohybrids co-doped by N and their enhanced photocatalytic ability, *J. Solid State Chem.* 192 (2012) 305–311.
- [10] S V. Trevisan, A. Olivo, F. Pinna, M. Signoretto, F. Vindigni, G. Cerrato, C.L. Bianchi, Investigation on the Stability of Supported Gold Nanoparticles, *App. Catal. B*, in press.
- [11] M.I. Litter, Heterogeneous photocatalysis: Transition metal ions in photocatalytic systems, *App. Catal. B: Environ.* 23 (1999) 89–114.
- [12] M. Ni, M.K.H. Leung, D.Y.C. Leung, K. Sumathy, A review and recent developments in photocatalytic water-splitting using TiO<sub>2</sub> for hydrogen production, *Sustain. En.Rev.* 11 (2007) 401–425.
- [13] D.L. Liao, C.A. Badour, B.Q. Liao, Preparation of nanosized TiO<sub>2</sub>/ZnO composite catalyst and its photocatalytic activity for degradation of methyl orange, *J.Photochem.Photobiol.* 194(2008) 11–19.
- [14] S. Bai, H. Li, Y. Guan, S. Jiang, The enhanced photocatalytic activity of CdS/TiO<sub>2</sub> nanocomposites by controlling CdS dispersion on TiO<sub>2</sub> nanotubes, *App. Surf. Sci.* 257(2011) 6406–6409.
- [15] B. Neppolian, A. Bruno, C.L. Bianchi, M. Ashokkumar, Graphene oxide based Pt–TiO<sub>2</sub> photocatalyst: Ultrasound assisted synthesis, characterization and catalytic efficiency, *Ultras. Sonochem.* 19 (2012) 9–15.
- [16] D.S. Bhatkhande, V.G. Pangarkar, A.A.C.M. Beenackers, Photocatalytic degradation using TiO<sub>2</sub> for environmental applications – A review, *J. Chem. Technol. Biotechnol.* 77 (2002) 102–116.

- [17] C. Ooka, H. Yoshida, M. Horio, K. Suzuki, T. Hattori, Adsorptive and photocatalytic performance of TiO<sub>2</sub> pillared montmorillonite in degradation of endocrine disruptors having different hydrophobicity, *App. Catal. B: Environ.* 41 (2003) 313–321.
- [18] Z.M. Xie Chen, Y. Z. Dai, Preparation of TiO<sub>2</sub>/sepiolite photocatalyst and its application to printing and dyeing wastewater treatment, *Environ. Sci. Technol.* 32(2009) 123-127.
- [19] Z. Sun, Y. Chen, Q. Ke, Y. Yang, J. Yuan, Photocatalytic degradation of a cationic azo dye by TiO<sub>2</sub>/bentonite nanocomposite, *J. Photochem. Photobiol. A: Chem.* 149(2002)169-174.
- [20] M. N. Chong, V. Vimonses, S. Lei, B. Jin, C. Chow, C. Saint, Synthesis and characterization of novel titania impregnated kaolinite nano-photocatalyst, *Micropor. Mesopor. Mater.* 117(2009) 233-242.
- [21] M. Mahalakshmi, S. Vishnu Priya, B. Arabindoo, M. Palanichamy, V. Murugesan, Photocatalytic degradation of aqueous propoxur solution using TiO<sub>2</sub> and H<sub>β</sub> zeolite-supported TiO<sub>2</sub>, *J. Haz. Mater.* 161 (2009) 336–343.
- [22] Y. Kameshima, Y. Tamura, A. Nakajima, K. Okada, Preparation and properties of TiO<sub>2</sub>/montmorillonite composites, *App. Clay Sci.* 45 (2009) 20-23.
- [23] G. Grubert, M. Wark, N. I. Jaeger, G. Schulz-Ekloff, O. P. Tkachenko, Reduction kinetics of zeolite-hosted mono- and polynuclear titanium oxide species followed by UV/Vis diffuse reflectance spectroscopy: influence of location and coordination, *J. Phys. Chem. B* 102 (1998) 1665–1671.
- [24] L. Xiang, X. Zhao, Preparation of montmorillonite/titania nano-composite and enhanced electro-rheological activity, *J. Colloid. Inter. Sci.* 296 (2006) 131–140.

- [25] J. Liu, X. Li, S. Zuo, Y. Yu, Preparation and photocatalytic activity of silver and TiO<sub>2</sub>nanoparticles/montmorillonite composite, *App. Clay Sci.* 37(2007) 275–280.
- [26] M. Judit, K. László, E. Bazsó, Z. Volker, R. André, D. Imre, Photocatalytic oxidation of organic pollutants on titania–clay composites, *Chemosphere* 70 (2008) 538–542.
- [27] P.T. Hang, G. W. Brindley, Methylene blue absorption by clay minerals. Determination of surface areas and cation exchange capacities (clay-organic studies XVIII), *Clays and Clay Miner.* 18 (1970) 203-212.
- [28] G. Cerrato, L. Marchese, C. Morterra, Structural and morphological modifications of sintering microcrystalline TiO<sub>2</sub>: an XRD, HRTEM and FTIR Study, *Appl. Surf. Sci.* 70/71 (1993) pp. 200-205
- [29] E. Rossetto, D.I. Petkowicz, J. H. Z. dos Santos, S. B. C. Pergher, F. G. Penha, Bentonites impregnated with TiO<sub>2</sub> for photodegradation of methylene blue, *Appl. Clay Sci.* 48 (2010) 602–606.
- [30] Y. Li, J. R. Liu, S. Y. Jia, J. W. Guo, J. Zhuo, P. Na, TiO<sub>2</sub> pillared montmorillonite as a photoactive adsorbent of arsenic under UV irradiation, *Chem. Eng. J.* 191 (2012) 66–74.
- [31] L.H. Little, *Infrared Spectra of Adsorbed Species*, Academic Press. London (1966).
- [32] C. Morterra, An infrared spectroscopic study of anatase properties. Part 6.—Surface hydration and strong Lewis acidity of pure and sulphate-doped preparations, *J. Chem. Soc.* 84 (1988) 1617–1637.
- [33] C. Morterra, V. Bolis, E. Fiscaro, The hydrated layer and the adsorption of CO at the surface of TiO<sub>2</sub> (anatase), *Colloids Surf.* 41 (1989) 177–188.

- [34] A. P. Legrand, *The Surface Properties of Silicas*, John Wiley and Sons. New York (1998).
- [35] G. Busca, V. Lorenzelli, Infrared spectroscopic identification of species arising from reactive adsorption of carbon oxides on metaloxide surfaces, *Mater. Chem.* 7 (1982) 89–126.
- [36] B. Z. Lin, X. L. Li, B. H. Xu, Y. L. Chen, B. F. Gao, X. R. Fan, Improved photocatalytic activity of anatase TiO<sub>2</sub>-pillared HTaWO<sub>6</sub> for degradation of methylene blue, *Micropor. Mesopor. Mater.* 155 (2012) 16–23.
- [37] B. Dou, H. Chen, Y. Song, C. Tan, Synthesis and characterization of hetero-structured nanohybrid of MgO-TiO<sub>2</sub>-Al<sub>2</sub>O<sub>3</sub>/montmorillonite, *Mater. Chem. Phys.* 130 (2011) 63– 66.
- [38] S.J. Gregg, K. S. W. Sing, *Adsorption, Surface Area and Porosity*, Academic Press London. (1992).
- [39] I. Fatimah, S. Wang, K. Wijaya, Composites of TiO<sub>2</sub>-aluminum pillared montmorillonite: synthesis, characterization and photocatalytic degradation of methylene blue, *App. Clay Sci.* 50 (2010) 588–593.
- [40] G. Kahr, F.T. Madsen, Determination of the cation exchange capacity and the surface area of bentonite, illite and kaolinite by methylene blue adsorption, *Appl. Clay. Sci.*, 9 (1995) 327-336.
- [41] A. Fernandez-Nieves, C. Richter, F.J. de las Nieves, Point of zero charge estimation for a TiO<sub>2</sub>/water interface, *Prog. Colloid Sci.*, 110 (1998) 21-24.
- [42] J. Liu, M. Dong, S. Zuo, Y. Yu, Solvothermal preparation of TiO<sub>2</sub>/montmorillonite and photocatalytic activity, *App. Clay Sci.* 43 (2009) 156–159.
- [43] J. Matos, A. Garcia, T. Cordero, J.-M. Chovelon, C. Ferronato, Eco-friendly TiO<sub>2</sub>-AC photocatalyst for the selective photooxidation of 4-Chlorophenol, *Catal. Lett.* 130 (2009) 568-574.